

# UPWARD FLOW AND HEAT TRANSFER AROUND TWO HEATED CIRCULAR CYLINDERS IN SQUARE DUCT UNDER AIDING THERMAL BUOYANCY

**H. Laidoudi**

Laboratory of Sciences and Marine Engineering (LSIM), Faculty of Mechanical Engineering,  
USTO-MB University, BP 1505, El-Menaouar, Oran 31000, Algeria  
e-mail: houssem.laidoudi@univ-usto.dz

## Abstract

This paper presents a numerical investigation of mixed convection heat transfer around a pair of identical circular cylinders placed in side-by-side arrangement inside a square cavity of single inlet and outlet ports. The investigation provided the analysis of gradual effect of aiding thermal buoyancy on upward flow around cylinders and its effect on heat transfer rate. For that purpose, the governing equations involving continuity, momentum and energy are solved using the commercial code ANSYS-CFX. The distance between cylinders is fixed with half-length of cavity. The simulation is assumed to be in laminar, steady, incompressible flow within range of following conditions:  $Re = 1$  to  $40$ ,  $Ri = 0$  to  $1$  at  $Pr = 0.71$ . The main obtained results are shown in the form of streamline and isotherm contours in order to interpret the physical phenomena of flow and heat transfer. The average Nusselt number is also computed and presented. It was found that increase in Reynolds number and/or Richardson number increases the heat transfer. Also, aiding thermal buoyancy creates new form of counter-rotating zones between cylinders.

**Keywords:** Mixed convection, circular cylinder, square cavity, aiding buoyancy, local Nusselt number, average Nusselt number.

## 1. Introduction

The flow inside a square cavity of single inlet and outlet ports where there are confined cylinders has tremendous engineering applications such as electronic cooling systems, heat transfer, heat exchangers, chemical application, and so on. Flow analyses around those cylinders are a first imperative step that can provide the initial required parameters used for the design and development of those systems. Generally, the required parameters summarize the flow mechanical phenomena and their impact on heat transfer rate such as local Nusselt number, average Nusselt number, drag coefficient...

Recently, some experimental and numerical researches were emphasized on the study of natural, forced and mixed convection inside a square enclosure under different range of fluidic and thermal controlling parameters.

(Darzi et al. 2017) numerically studied the mixed convection through a laminar flow inside enclosure cavity where there are two heated circular cylinders of different locations. The flow is

driven by the top cold lid while the other walls are stationary and adiabatic. The governing equations are solved by employing the Boltzmann method. The main purpose of this study is to looking for optimal arrangement of cylinders. The obtained results indicated that for all geometrical configurations of cylinders, an increase in Richardson number increases the heat transfer. Also, the optimal arrangement of cylinders is when the cylinders are closed to the top section of cavity. This optimal configuration is characterized with highest value of average Nusselt number. (Mishra et al. 2017) studied the forced convection around a two circular cylinders of two geometrical configurations one when the cylinders are placed in side-by-side arrangement and the second when the cylinders are placed in tandem arrangement. (Karimi et al. 2016) numerically investigated the mixed convection around two heated horizontal cylinders located in square to-dimensional enclosure. The purpose of this research is to analyze the effects of cylinder diameter, Reynolds number and Richardson number on heat transfer characteristics. (Chatterjee and Halder 2014) studied the heat transfer around a two rotating circular cylinders located inside square enclosure. (Talkhoncheh et al. 2016) performed in unsteady laminar regime a flow of Newtonian fluid and forced convection heat transfer around cylinders situated inside a square cavity of single inlet and outlet ports. It was found that when  $Re$  was less than 460, the effect of space between cylinders was found to be nearly negligible. (Chatterjee and Gupta 2014) carried out in two-dimensional simulations the effect of hydromagnetic mixed convective transport in a nonisothermally heated vertical lid-driven square enclosure filled with an electrically conducting fluid in the presence of a heat-conducting solid circular cylinder. (Park et al. 2012) studied natural convection inside square enclosure with hot and cold cylinders. The work is done in two-dimensional simulations. The study showed the influence of Rayleigh number ranging between  $Ra = 10^3$  and  $10^5$ . (Prasard and Koseff 1996) experimentally analyzed the mixed convection heat transfer in lid driven cavity for many different values of Richardson number. (Mehrizi et al. 2013) and (Parvin et al. 2012) have studied also the same thematic.

From the above survey, it was concluded that when the flow pass around cylinders which are located inside cavity, many different kind of recirculation zone appeared inside the cavity. The position as well as size of recirculation zones depends on large number of parameters, such as the location of inlet and outlet ports (Sourtiji et al. 2011), the influence of thermal buoyancy (Mamun et al. 2010), the position and number of obstacle cylinders inside the cavity (Boulahia et al. 2017), fluid proprieties and heat transfer characteristics (Karbasifar et al. 2018).

Based on these literatures, no attention has been focused to gradual effect of aiding thermal buoyancy on fluid flow and heat transfer of a circular cylinders placed in side-by-side within a square cavity of single inlet and outlet ports. Therefore, this paper tries to fill the gap in literature. The purpose of this work is to study numerically the gradual effect of thermal buoyancy around circular cylinders located inside square enclosure. The obtained results are presented and discussed for the range of following conditions:  $Re = 1$  to 40,  $Ri = 0$  to 1 at fixed value of  $Pr = 0.71$ .

## 2. Physical model and governing equations

Fig. 1 shows schematically the geometrical configuration taken into account in this paper. It was selected from the previous investigation of (Mishra et al. 2017). As it is illustrated in Fig. 1, two heated circular cylinders of diameter ( $d$ ) placed in side-by-side arrangement at the centre of square cavity of side ( $L$ ). The gap distance between the cylinders is fixed at  $S = 0.5L$ . The square cavity contains an inlet port situated at lower-middle wall and an outlet port situated upper-middle wall of cavity, the width of each ports is equal  $l = 0.1L$ . The diameter of each cylinder,  $d$  is fixed at the value  $d = 0.1L$ . The main object of this research is to compute numerically the flow of Newtonian fluid inside this cavity of adiabatic walls and predict exactly the effect of thermal

buoyancy. Therefore, due to computational considerations, the flow enters the cavity through lower-middle port with uniform velocity ( $u_{in}$ ) and constant temperature ( $T_{in}$ ), and passes the cylinders, whose surfaces are maintained at constant temperature  $T_w$ , ( $T_w > T_{in}$ ), then leaves the cavity through upper-middle port.

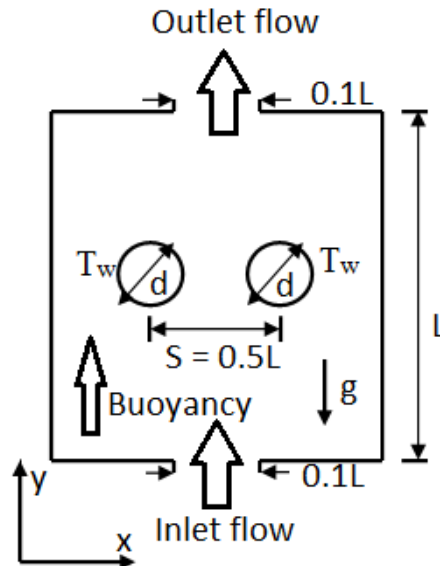


**Fig.1.** Schematic presentation of the flow over two cylinders inside a square enclosure of inlet and outlet ports

The global equations defining the thermal buoyancy and its effect on fluid flow and heat transfer can be written based on the conservation of mass, momentum and energy. For present work, the governing equations are assumed to be solved in 2D for laminar, steady and incompressible flow. The thermo-physical properties of studied fluid are assumed to be independent of temperature except for the density appearing in the body force term in y-momentum equation showing the influence of aiding thermal buoyancy. The evolution of density and temperature is defined according to Boussinesq approximation with negligible viscous dissipation. Finally, the governing equations can be written mathematically in dimensionless form as follows:

$$\frac{\partial U}{\partial X} + \frac{\partial V}{\partial Y} = 0 \quad (1)$$

$$U \frac{\partial U}{\partial X} + V \frac{\partial U}{\partial Y} = -\frac{\partial P}{\partial X} + \frac{1}{Re} \left( \frac{\partial^2 U}{\partial X^2} + \frac{\partial^2 U}{\partial Y^2} \right) \quad (2)$$

$$U \frac{\partial V}{\partial X} + V \frac{\partial V}{\partial Y} = -\frac{\partial P}{\partial Y} + \frac{1}{Re} \left( \frac{\partial^2 V}{\partial X^2} + \frac{\partial^2 V}{\partial Y^2} \right) + Ri\theta \quad (3)$$

$$U \frac{\partial \theta}{\partial X} + V \frac{\partial \theta}{\partial Y} = \frac{1}{PrRe} \left( \frac{\partial^2 \theta}{\partial X^2} + \frac{\partial^2 \theta}{\partial Y^2} \right) \quad (4)$$

The dimensionless variables that are written in above equation can be written:

$$(X, Y) = \frac{(x, y)}{d}, (U, V) = \frac{(u, v)}{u_{in}}, P = \frac{p}{\rho u_{in}^2}, \theta = \frac{(T - T_{in})}{T_w - T_{in}} \quad (5)$$

where  $U, V$  are dimensionless velocity components along  $X, Y$  directions, respectively,  $P$  and  $\theta$  are dimensionless pressure and dimensionless temperature of fluid, respectively.

Reynolds number ( $Re$ ), Grashof number ( $Gr$ ), Richardson number ( $Ri$ ), Prandtl number ( $Pr$ ) are defined respectively as follows:

$$Re = \frac{u_{in} d}{\nu}, Gr = \frac{g \beta_T \Delta T d^3}{\nu^2}, Ri = \frac{Gr}{Re^2}, Pr = \frac{\nu}{\alpha} \quad (6)$$

Where  $u_{in}, \alpha, g, \nu, \beta_T$  are inlet velocity flow, thermal diffusivity, gravitational acceleration, kinematic viscosity, and volume expansion coefficient, respectively.

The appropriate boundary conditions for this work can be identified as follows:

At the inlet port (lower-middle port): uniform velocity and constant temperature, i.e.,

$$U = 0, V = 1, \theta = 0 \quad (7)$$

At the outlet port (upper-middle port): Neumann boundary condition is used for flow velocity and temperature, i.e.,

$$\frac{\partial U}{\partial X} = 0, \frac{\partial V}{\partial X} = 0, \frac{\partial \theta}{\partial X} = 0 \quad (8)$$

On cylinder surface: no-slip condition and constant temperature, i.e.,

$$U = 0, V = 0, \theta = 1 \quad (9)$$

On the cavity walls: no-slip flow with adiabatic condition, i.e.,

$$U = 0, V = 0, \frac{\partial \theta}{\partial n} = 0 \quad (10)$$

where  $n$  is the normal direction to cavity walls.

The local Nusselt number on cylinder surface is obtained by the expression:

$$Nu_l = \frac{hd}{k} = -\frac{\partial \theta}{\partial n_s} \quad (11)$$

where  $h, k$  and  $n_s$  are the local surface heat transfer coefficient, thermal conductivity of the fluid and the normal direction to the cylinder surface, respectively. These local values on entire surface were then averaged to obtain the average Nusselt number of cylinder.

$$Nu = \frac{1}{S} \int_s Nu_l ds \quad (12)$$

The Nusselt number is calculated after knowing the distribution of temperature across the cylinder surface.

### 3. Numerical procedure

The numerical solution of governing equations for present research is performed by ANSYS-CFX package which is developed by AEA technology. ANSYS-CFX utilizes finite volume methods to solve numerically the main governing equations subjected to appropriate boundary conditions. The principal methodology of this code is to convert the governing partial differential equations of momentum, continuity and energy into a system of discrete algebraic equations by discretizing the entire numerical domain. For present work, the flow is assumed to be steady-state and laminar. The internal effect of aiding thermal buoyancy on fluid flow is added to system as source term in momentum equation (y-direction) through (Function) feature of ANSYS-CFX. The high resolution discretization scheme is used for the spatial discretization of the convective terms, (SIMPLEC algorithm) a pressure-correction method of the type Semi-Implicit Method for Pressure- Linked Equations-Consistent is used as the pressure-velocity coupling scheme. The convergence criteria based on relative error for the inner iterations are set as  $10^{-8}$  for the discretized continuity and momentum equations and  $10^{-6}$  for the discretized energy equation.

Fig.2 shows the state of grid distributions used for this work. As it is shown, a triangular unstructured grid points with non-uniform distributions around cylinders are generated. The grid points are observed to have a close clustering of grid points around the walls of cylinders. This mesh was generated by the package called Gambit software. This paper incorporates also the section of the grid independency test to proof the accuracy of chosen grid. For that reason, four different mesh sizes are generated separately (Mesh1 = 60974, Mesh2 = 132958, Mesh3 = 315168 and Mesh4 = 621664 cells). The checking test is executed with the respect to average Nusselt number ( $Nu$ ) of each cylinder for Reynolds number of  $Re = 20$  and Richardson number of  $Ri = 0$  at Prandtl number of  $Pr = 1$ . Table 1 presents all mesh cells and their obtained values of average Nusselt number. CN, shown in Table 1 indicates the number of nodes on cylinder wall of each grid. The analyze of Table 1 shows that the minimum difference of Nusselt number is between (Mesh3) and (Mesh4), it is about 0.043%. Therefore, Mesh3 can be considered as the best mesh for the rest of present work.

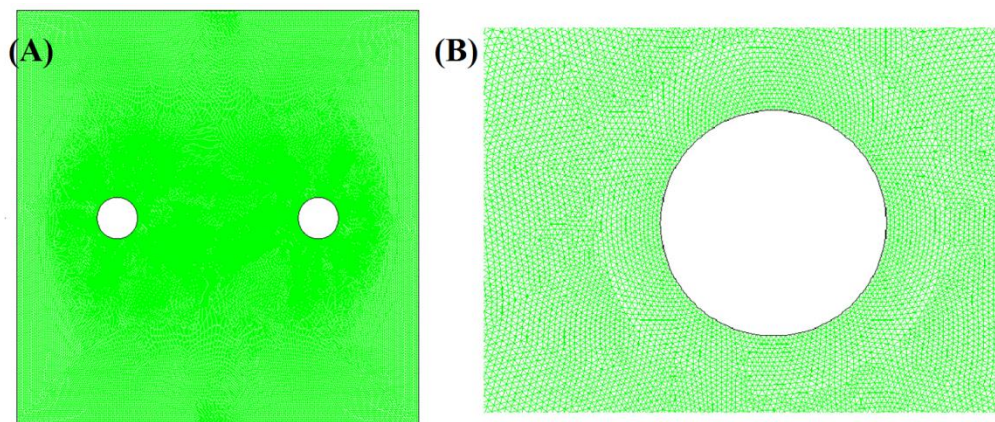


**Fig.2.**Grid distribution (a) in whole computational domain, and (b) a closer view around cylinder

**Table 1.** Details of grid independency test

Mesh	Elements	CN	$Nu$
Mesh1	60974	100	0.695508
Mesh2	132958	150	0.756507
Mesh3	315168	250	0.259637
Mesh4	621664	350	0.259751

#### 4. Results and discussion

The steady 2D numerical simulations were carried out within the range of following conditions:  $Re = 1$  to 40,  $Ri = 0$  to 1 at fixed value of Prandtl number  $Pr = 0.71$  and blockage ratio  $\beta = d/L = 0.1$ . The main results of this work are illustrated and discussed in terms of streamlines, isotherms and average Nusselt number. The studied domain can be encountered in many different engineering applications such as exchangers, electronic cooling systems, building ventilation... Also, the obtained values of average Nusselt number can be used in design and development of such geometries. Analyses of new results are presented in this section, but prior to that, some compared results are well presented here in order to examine the accuracy and the reliability of present numerical methodology.

##### 4.1. Validation of the numerical solution methodology

In order to examine the precision of our numerical methodology, some comprehensive tests are performed to verify and to evaluate the accuracy of present results in comparison with other previous results. Table 2 shows the results of validation test, i.e. average Nusselt number of two square cylinders placed in tandem arrangement within a two parallel walls in the range of conditions:  $Re = 1$  to 30 at  $Ri = 0.25$  and  $Pr = 10$ . A good agreement is observed between the present results and the previous results reported in the literature. The Fig. 3 shows streamlines comparison between present result and the result of (Mishra et al. 2017). A good agreement also is observed between the results.

**Table 2.** Validation test

$Re$	First cylinder			Second cylinder		
	$Nu$	$Nu$ (Chatterjee et al. 2010)	Error %	$Nu$	$Nu$ (Chatterjee et al. 2010)	Error %
1	1.79	1.8	0.56	1.26	1.3	3
10	3.94	3.94	0	2.59	2.6	0.4
30	6.37	6.4	0.47	3.78	3.83	1.3

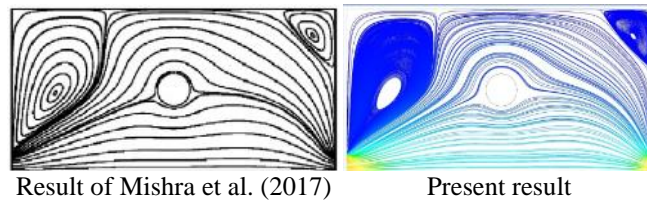


**Fig. 3.** Streamlines comparison between present result and that of Mishra et al. (2017) for  $Re = 5$  and  $Ri = 0$

#### 4.2. Streamlines and isotherm contours

It is known that the visualization of streamlines and isotherms gives the detailed information about the flow kinematic which delineates counter-rotating/stagnant regions and/or local spot temperatures. Also, certain engineering applications require the homogenization of the fluid flow. For that purpose, Figs. 4 and 5 respectively depict representative streamlines and isotherm contours for different values of Reynolds and Richardson numbers at fixed values of Prandtl number and blockage ratio. From Fig. 4 it is observed that for  $Ri = 0$  (no effect of thermal buoyancy) two cellular vortices appear just at the left and right of inlet port. This effect is due to sudden expansion of the flow which engenders sudden changes of flow direction. The same phenomena are observed at the outlet port, but in this case the vortices are located in the enclosure corners. The size of both vortices of inlet and outlet are observed to be increased along stream-wise and transverse with the gradual increase in Reynolds number at the point that they are associated. This behavior can be explained by the fact that increase in the value of Reynolds number increase the fluid inertia and therefore, the fluid gradually loses the ability to follow sudden changes in flow direction. Interesting evolution of vortex sizes are observed with the respect to thermal buoyancy strength. At fixed Reynolds number, increased Richardson number decreases the vortex sizes. At the lower value of Reynolds number ( $Re = 1$ ), the thermal buoyancy has a tendency to suppress completely the inlet vortices. This can be attributed by the fact that the increase in the value of Richardson (i.e., the buoyancy becomes more effected) the velocity of fluid particles in vicinity of cylinders increases and moves toward the upper enclosure wall. Consequently, the vortex sizes reduce and the stability of the flow increases.



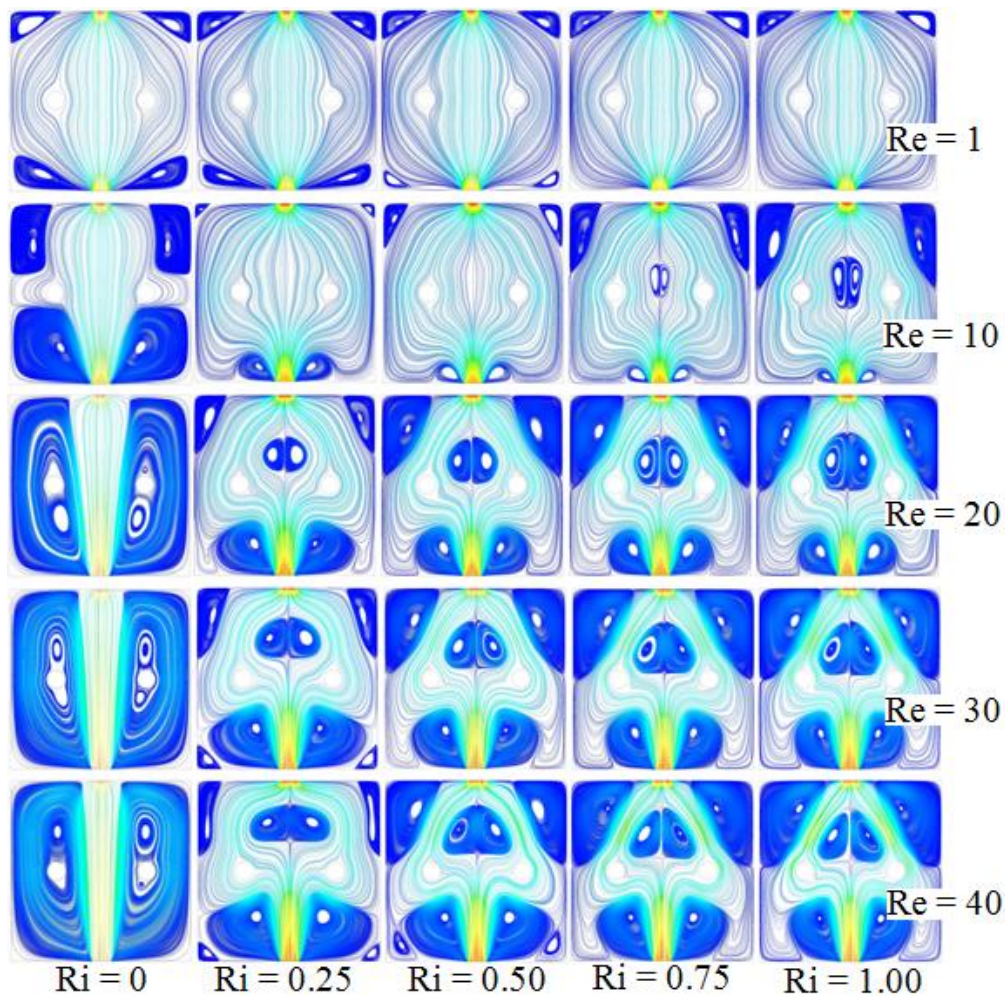


**Fig. 4.** Representative streamlines for side-by-side arrangement of cylinders for different values of Reynolds number and Richardson number

It is also observed that another closed steady recirculating spot containing of twin symmetric vortices appears between the cylinders. The size of the bubbles is observed to be increased by increasing Richardson and/or Reynolds numbers. The appearance of vortices is due to the difference of pressure between vicinity of heated obstacle surfaces and the surface between cylinders where it is colder. Accordingly, the pressure gradient creates a counter-rotating flow between cylinders.

Fig.5 presents the effect of Reynolds number and Richardson number on the isotherms at fixed value of Prandtl number and blockage ratio. For  $Ri = 0$ , such structure of thermal plumes are observed to be formed around the cylinders. For each value of Reynolds number the plume directions around the cylinders are directed toward the zones of cellular vortices as it was shown in streamlines. When the thermal buoyancy is superimposed, it is observed that the isotherm crowding around the cylinders and especially at the front surfaces increase with increasing Richardson number, this behavior indicates the increment of heat transfer rates. The isotherms for  $Re = 1$  are similar for all values of  $Ri$  due to the low value of flow velocity. Furthermore, the



isotherm profiles are directed toward outlet port with gradual increase in buoyancy strength. Also, the lateral spread of profiles is progressively reduced with increase in the effect of aiding buoyancy. Finally, based on isotherms it can be predicted that increase in aiding buoyancy strength enhances the heat transfer rates of cylinders.

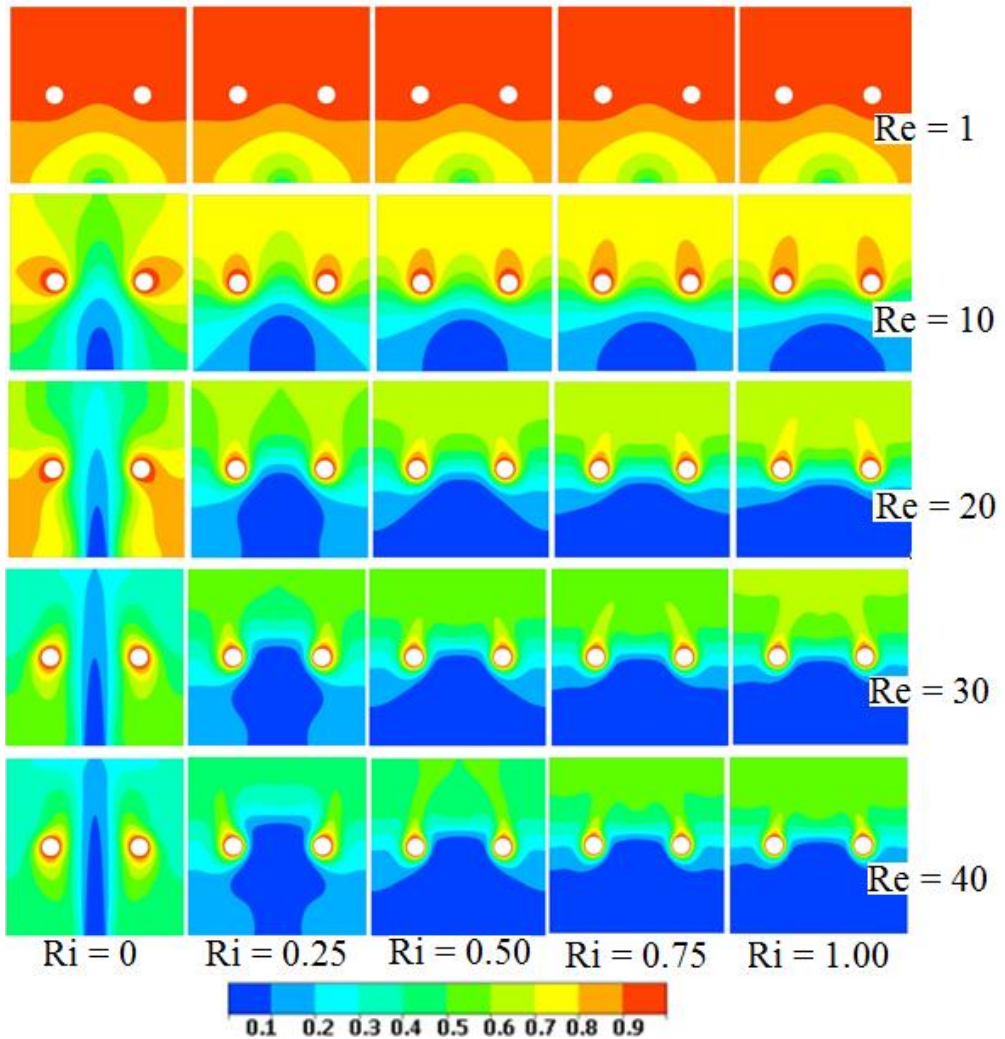


**Fig. 5.** Representative isotherms for side-by-side arrangement of cylinders for different values of Reynolds number and Richardson number

#### 4.3. Average Nusselt number

Fig.6 depicts the variations of average Nusselt number along the cylinder surface with Reynolds number for different values of Richardson number. Fig. 6 indicates that the average Nusselt number depends positively on Reynolds number for all values of Richardson number. Also, an increase in Richardson number increases the average Nusselt number. It is also observed that the effect of Richardson number on average Nusselt number becomes more significant for the gradual increase in of Reynolds number.

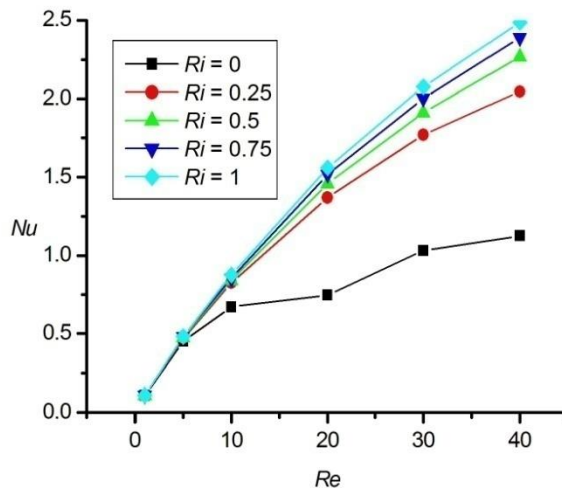


**Fig. 6.** Variation of average Nusselt number with Reynolds number for different values of Richardson number

## 5. Conclusion

This paper presented a computational research of the gradual effect of aiding thermal buoyancy strength and Reynolds number on upward flow and mixed convection heat transfer of viscous fluid around two heated cylinders placed in side-by-side arrangement inside a square enclosure of single inlet and outlet ports. The obtained results of flow patterns and temperature distribution are mainly presented in terms of streamlines and isotherm contours in order to understand the physical insights of flow nature. The flow instability was seen to be increased with increasing Reynolds number. Furthermore, the aiding thermal buoyancy has a tendency to decrease flow instability. It was also seen that for present studied geometry, the aiding buoyancy formed two similar vortices between the cylinders. Moreover, the average Nusselt number increases with an increase in Reynolds number and/ or Richardson number. Finally, it can be concluded that using aiding thermal buoyancy thermal process can be more beneficial than using only pure convection.

## References

- Boulahia Z, Wakif A, Chamkha A J, Sehaqui R (2017). Numerical study of natural and mixed convection in a square cavity filled by a Cu–water nanofluid with circular heating and cooling cylinders. *Mechanics & Industry*. 502:1-21.
- Chatterjee D., Amiroudine S. (2010). Two-Dimensional mixed convection heat transfer from confined tandem square cylinder in cross-flow at low Reynolds number, *Int. Comm. in Heat and Mass Transfer*. 37: 7-16.
- Chatterjee D, Halder P (2014). MHD mixed convective transport in square enclosure with two rotating circular. *Numerical Heat Transfer*. 65: 802-824.
- Chatterjee D, Gupta SK (2014). Hydromagnetic mixed convective transport in a nonisothermally heated lid-driven square enclosure including a heat-conducting circular Cylinder. *Industrial & Engineering Chemistry Research*. 53 (51): 19775-19787.

- Darzi AAR, Eisapour AH, Abazarian A, Hosseinnajad F, Afrouzi HH (2017). Mixed convection heat transfer analysis in an enclosure with two hot cylinders: A Lattice Boltzmann Approach. *Heat Transfer-Asian Research*. 46 (3):218-236.
- Karbasifar B, Akbari M, Toghraie D (2018). Mixed convection of Water-Aluminum oxide nanofluid in an inclined lid-driven cavity containing a hot elliptical centric cylinder. *Heat and Mass Transfer*. 116: 1237-1249.
- Karimi F, Xu H, Wang Z, Yang M, Zhang Y (2016). Numerical simulation of steady mixed convection around two heated circular cylinders in a square enclosure. *Heat Transfer Engineering*. 37 (1): 64-75.
- Mamun M A H., Rahman M M, Billah M M, Saidur R (2010). A numerical study on the effect of a heated hollow cylinder on mixed convection in a ventilated cavity. *Communication in Heat and Mass Transfer*. 37: 1326-1334.
- Mehrizi AA, Farhadi M, Afrouzi HH, Shayamehr S (2013). Lattice Boltzmann simulation of natural convection flow around a horizontal cylinder located beneath an insulation plate. *Theor Appl Mech*. 51 (3):729-739.
- Mishra L, Baranwal A.K., Chhabra R P (2017). Laminar forced convection in power-law fluids from two heated cylinders in a square duct. *Heat and Mass Transfer*. 113: 589-612.
- Park Y G, Yoon H S, Ha M Y (2012). Natural convection in square enclosure with hot and cold cylinders at different vertical locations. *Heat and Mass Transfer*. 55:7911-7925.
- Parvin S, Alim M A, Hossain N F (2012). Prandtl number effect on cooling performance of a heated cylinder in an enclosure filled with nanofluid. *Communication in Heat Mass Transfer*. 39: 1220-1225.
- Prasad A K, Koseff J R (1996). Combined forced and natural convection heat transfer in a deep lid-driven cavity flow. *Heat Fluid Flow*. 17: 460-467.
- Sourtiji E, Hosseinnazadeh S F, Gorji-Bandpy M, Ganji D D (2011). Heat transfer enhancement of mixed convection in a square cavity with inlet and outlet ports due to oscillation of incoming flow. *Communication in Heat and Mass Transfer*. 38: 806-814.
- Talkhoncheh F K, Xu H, Wang Z, Yang M (2016). Numerical simulation of transient forced convection in a square enclosure containing two heated circular cylinders. *Numerical Methods for Heat and Fluid Flow*. 26(1): 307-327.